NONDESTRUCTIVE TESTING AND RESIDUAL STRESS MEASUREMENT IN CERAMICS USING X-RAY METHOD

Shun-ichiro Tanaka

New Materials Engineering Laboratory, Toshiba Corporation
2-4, Suehiro-cho, Tsurumi-ku, Yokohama, 230 Japan

ABSTRACT

Two recent topics on X-ray nondestructive evaluation are overviewed and discussed from the view point of a tool to check and confirm the reliability of structual ceramics. One is high sensitive and high speed 3rd generation X-ray CT scanner testing which can detect the inner defects/flaws in ceramics. Its detectability in ceramics was 200 μm for void, 20 μm in thickness for cracks in graphite and 1 % for density difference, X-ray CT NDE was also applied to crack detection in joined

Si3N4/metal. Another is direct measurements of residual stress at a confined area using <0.3mm collimated Cr Kα beam which enables to evaluate its detailed distribution quantitatively and nondestructively around ceramics/metal joined interface. Residual stress distribution of axial and along the interface were measured in Si3N4/Cu/steel to compare with FEM analysis. It was newly revealed that residual normal stress, σ_{Ry}, along the interface reached maximum tensile at the center of joint which could be analysed as the three dimensional effect. At the region of 0.5-1.0 mm from the corner edge, steep stress drop by Cu buffer local yielding was also measured.

1.INTRODUCTION

Among key items to the ceramics application as mechanical/electrical components, nondestructive evaluation technologies of imperfection and residual stress could be most important from the practical points of view.

As ceramics is brittle materials, it is very sensitive to both inner and surface defects/flaws. Statistically, the diameter of most frequent crack(void) for fracture origin of Si3N4 was 30 - 50 μm. To keep reliability in the ceramic components, it is necessary to detect the spatial positions and dimensions of such defects quantitatively. Nondestructive testing methods of ceramics are categorized into the following items by the physical media of testing ; the optical ones (VT, PT), the ultrasonic ones (including AE) and the testing

using radioactive rays such as X-ray. Developments in the technologies of radiography and computed tomography (CT) have made X-ray the powerful tool of ceramic nondestructive evaluation.

Residual stress has also been the important factor which affects on the mechanical strength of bulk or joined ceramics. Though conventional methods, such as indentation, ultrasonic microscope and laser speckle, have been developed for residual stress measurement, only X-ray enables to measure it nondestructively and quantitatively. Moreover, detail distribution of actual residual stress can be evaluated by the collimated X-ray directly to compare with FEM analysis.

In this paper, two recent topics on X-ray nondestructive evaluation are overviewed and discussed from the view point of a tool to check and confirm the reliability of structual ceramics.

2.NONDESTRUCTIVE TESTING BY X-RAY CT SCANNER

As the three dimentional information inside a body should be required with high accuracy and within the shortest possible time, the computed tomography technologies has been naturally combined with the highly penetrative X-ray radiation. Other types of CT methods utilizing high energy sources such as γ-ray or neutron, or NMR, ultrasonic waves or thermic rays have also been developed, but none is superior to the one utilizing X-ray as far as efficiency and accuracy in detecting flaws is concerned.

Industrial X-ray CT scanner which has been developed from medical field is now widely applying as the quality inspection tool to the machinery, automobile, aircraft/spacecraft and food/agriculture industry. For industries in which ceramics are applied, however, the detectability should be increased up to 50 μm because of high sensitivity to the flaws in brittle materials.

Presented below are medium energy type of industrial X-ray CT, its performance and application to ceramic components[1].

2-1. Specifications of industrial X-ray CT

There are two types of X-ray CT scanner as the practical third generation modes ; "TOSCANER 3000 Series of medium energy high speed type and "TOSCANER 4000 Series of high energy type. Specifications including detectability are presented in Table 1. 3000 Series are adequate for nondestructive inspection of materials made of light weight atom.They are Si_3N_4, SiC, Sialon, Al_2O_3, AlN and mullite for ceramics, and plastics, composite materials, and light alloys. On the other hand, 4000 Series are applicable to that made of heavy element such as ZrO_2, iron, steel and other metals, or to thick/large body.

The principle of the third generation CT scanner is shown in Fig. 1 schematically. As the penetrated X-ray images are detected by the multi-channel detector, they are digitized and easily processed to form clear CT reconstruction images which contain various beneficial

informations as shown in Fig. 2. Not only defects are detected and measured, density can also be measured and materials are identified from the X-ray absorption coefficient (CT number). CT number is defined as indicated in Fig, 3 and determined from the X-ray absorption coefficient assuming 0 for water and -1000 for air. It is nearly proportional to the density so that the density distribution can be determined from CT number. Minimum discernible difference in density was 1 %.

2-2. Flaw detectability in ceramics

Detectabilities of flaws in ceramics are also shown in Table 1 ; for voids 200 μm in diameter and for cracks 20 μm in width in the case of pixel (picture cell) size 300 μm[1]. Examples of crack detectability test for graphite is shown in Fig. 4. Artificial 20 μm slit was detected successfully. Cracks propagated into two tips in mullite component was also clearly shown in Fig. 5. Inclusions in ceramics which will be the fracture origins can be easily detectable using the difference of CT values.

X-ray CT is the useful tool to detect the imperfections around the joined ceramic/metal interfaces caused by thermal expansion mismatch. Fig. 6 shows the round cracks introduced from the Si3N4/Ti interface in the Si3N4/Ti/Mo system (Ti:buffer interlayer)[2]. Although these inner cracks was not visually observed, tomogram obtained by slicing at the position drawn in Fig. 6 enables us to know the three dimensional distribution of cracks around joined interface.

Combination with the other NDE technologies, such as ultrasonic C scan, might confirm their potentiality moreover[2].

3.RESIDUAL STRESS MEASUREMENT BY COLLIMATED X-RAY BEAM

For the actual application to components, ceramics is used with diamond wheel machining and with bonded to metal. These processes cause the residual stress to the ceramics, with which the mechanical strength is influenced. Especially, it is very important for ceramics/metal joined system because residual stress caused by thermal expansion mismatch between ceramics and metal will decrease bonding strength. In the extreme case, crack is introduced and propagated into ceramics when residual stress exceeds over its tensile strength. To relax the residual stress, plastic deformation of inserted ductile buffer metal, such as Cu or Ni, has been often used[3]. During cooling process, these metals can be easily deformed by the stress less than 100 MPa followed by decrease and relaxation of residual stress. From these practical reasons, the necessity to estimate the residual stress distribution around joined interface has been increasing. In this section, presented are recent results which I have successfully measured detailed residual stress distribution around joined interface by using collimated X-ray beam.[3]

3-1. Principles of residual stress measurement

The method to estimate the residual stress has been stress analysis using FEM or continuum theory of

mechanics. Since the analysed stress profiles depends on the model or boundary conditions, it is naturally hoped to evaluate and measure them directly. Though many measuring methods have been developed, X-ray method is recognized as the best one because it enables us to evaluate nondestructively and quantitatively. The principle of residual stress measurement is shown in Fig. 7. Residual stress is detected as diffracted X-ray peak shift which reflects the lattice spacing change by stress. And its value can be uniquely calculated by equation (1).

$$\sigma_R = -\frac{E}{2(1+\nu)} \cdot \cot\theta_0 \cdot \frac{\pi}{180} \cdot \frac{\partial(2\theta)}{\partial(\sin^2\psi)}$$

$$= K \cdot \frac{\partial(2\theta)}{\partial(\sin^2\psi)} \cdots\cdots\cdots\cdots (1)$$

where σ_R:residual stress, E:Young's modulus, ν:Poisson's ratio, θ_0:standard Bragg's angle, ψ:X-ray incident angle, K: stress constant.

Measured residual stress is obtained from the surface layer of materials which is easily understood in Fig. 7.

The application of X-ray method to metal has been popular. On the contrary, it has not been widely applied to ceramics because it is difficult to optimize the experimental conditions and because the irradiation area was too large to apply to the joined interfaces. In this study, detailed distribution of residual stress in the surface (about 20 μm in depth) of Si_3N_4 can be successfully measured by using highly powered and $\leq$ 0.3mmϕ collimated Cr Kα X-ray.

3-2. Residual stress distribution around joined interfaces

Surface residual stress distribution in Si3N4/Cu/steel joint was measured. Its distribution includes axial and along the joined interface to compare with FEM analysis. Joint was made by active metal brazing with 0.2 mm Cu buffer layer[4]. Specimen's structures was basically the same as that used in X-ray CT experiments (Fig. 6). The apparatus to measure residual stress was equipped with collimator and position sensitive proportional counter (PSPC) to get the detailed distribution in a short time. Measuring conditions are shown in Table 2.

The axial distributions of the residual stresses in the 3 X 4 X 40mm "GROUND" Si3N4/0.2tCu/steel rectangular joint are shown in Fig. 8(a). In Si3N4, the normal stress value in the y direction, σ_{Ry}, reached up to 250 MPa in tension at the position of 0.2 mm from the boundary, and then it decreased to zero and compressive stress appeared as the position moved away from the interface. This distribution coincided well with the result of FEM prediction and was obtained with small size X-ray collimation for the first time. The normal stress in the x direction, σ_{Rx}, changed inversely from compression to tension. The stress in the joined low carbon steel was compressive wherever measured[3].

The residual stress distributions along the interface were slightly different from that of two dimensional FEM calculation, as shown in Fig. 8(b)[3]. According to elastic or elasto-plastic two dimensional calculation, normal stress σ_{Ry} and maximum principal stress σ_1 reached

tensile maximum at the joined edge as a singularity point. Experimental results matched well at the edge, but not matched at the center position where maximum tensile stress was also observed. This results were exaggerated and confirmed in the same plate-like "LAPPED" joint, 3 X 30 X 40 mm, as shown in the Fig. 9[5]. In this specimen, finely collimated 0.1 mmϕ Cr-Kα beam was irradiated to Si3N4 on the line 0.1 mm close to the boundary to know the fine structure of residual stress distribution. At the edge, large tensile stress remained in both normal stress, σRy and σRx, while normal stress σRy showed larger maximum at the center position of plate specimen. Elastic three dimensional FEM analysis shows such maximum at the center position reasonably, in which the volumetric tensile effcts act on to the surface. In the region of 0.5-1.0 mm inside from the edge, steep stress drops were clearly observed in both σRy and σRx. These are the results of "local yielding effect" of ductile Cu buffer layer and could be analysed by elasto-plastic three dimensional analysis.

Measured residual stress values can be related to the bonding strength of Si3N4/steel joints. During bending testing, not only residual stress, but also stress concentration acts on the Si3N4/steel interface. Since both effects cause the strength degradation of monolithic Si3N4, the dependence of bending strength on the Cu layer thickness could be successfully explained by these two concepts[3].

4. CONCLUSIONS

Two recent topics on X-ray nondestructive evaluation are overviewed from the view point of a tool to check/confirm the reliability of ceramics and its joint. The results are summarized as follows:

4-1. Nondestructive testing by X-ray CT scanner

(1)Third generation X-ray CT scanner is a useful tool to detect inner defects of ceramics with which shape, position, defect mode and element can be identified.
(2)Detectability of defects/flaws in ceramics is 200 μm in diameter for void, 20 μm in thickness for cracks and 1 % for density difference.
(3)Cracks in Si3N4 propagated from interface was sensitively detected in Si3N4/steel joint.

4-2. Residual stress measurement by collimated X-ray beam

(1)Residual stress was successfully measured quantitatively and nondestructively at the confined region around Si3N4/Cu/steel joined interface using 0.1mmϕ collimated X-ray.
(2)Axial distribution of residual stress varied complexly within 2 mm range from interface which profile can be predicted by two dimensional FEM analysis.
(3)It was newly revealed that residual normal stress σ_{ry} along the interface reached maximum tensile at the center region of joint which could be analysed as the three

dimensional effcts by FEM calculation.

(4)At the corner edge, namely singularity point, normal and maximum principal stress showed large tensile stress, while steep stress drop was occured at 0.5-1.0 mm inside by Cu buffer local yielding effect.

REFERENCES

[1]Y.Tanimoto, S.Tanaka and M.Tomizawa, "Application of X-Ray CT Scanner to Nondestructive Testing"; Proc. Tokyo Int. Gas Turbine Congress (1987.10) Tokyo, p.I/155-161

[2]Shun-ichiro Tanaka and Ichiro Komura, "Nondestructive Evaluation of Ceramic/metal Joined System"; Abstract of Japan Institute of Metals Meeting (1988.4), p.356

[3]Shun-ichiro Tanaka, "Residual Stress Relaxation In Si3N4/metal Joined Systems"; Proc. MRS Int. Meeting on Advanced Materials (1988.5-6) Tokyo

[4]Shun-ichiro Tanaka, "The Characterization of Ceramic/Metal Systems Joined by An Active-Metal Brazing Method"; Proc. MRS Int. Meeting on Advanced Materials (1988.5-6) Tokyo

[5]Shun-ichiro Tanaka and Yumiko Takahashi, "Measurement of Residual Stress Distribution around Si3N4/Metal Interface by X-ray Method"; Abstract of Japan Institute of Metals Meeting (1989.4), p.153

Table 1. Specifications of industrial X-ray CT

Model / Specification	TOSCANER 3100	TOSCANER 3200	TOSCANER 4100	TOSCANER 4200
Scan system	. The third generation mode . Pulse X-ray 120 kV . Xe 512 ch . Scan	. The third generation mode . Pulse X-ray 140 kV . Xe 512 ch . Scan/scanno-gram	. The second generation mode . Continual X-ray 420 kV . Scintillator 8 ch . Scan	. Sector scan mode . Continual X-ray 420 kV . Scintillator 8 - 64 ch . Scan/scanno-gram
Penetra-bility	Equivalent to ø150 mm Aℓ	Equivalent to ø150 mm Aℓ	Equivalent to ø60 mm steel	Equivalent to ø60 mm steel
Minimum pixel size	300 μm	300 μm	250 μm	300 μm
Inspec-tion time	15 seconds	15 seconds	10 minutes	4 - 30 minutes
Scan field	ø150 mm	ϕ150/240/ 300 mm	ø50 mm	ø300/ 600 mm
Variable slice location	Semi-fixed	600 mm	100 mm	600 mm
Display and detecta-bility	. Display matrix : 320 x 320 . Detectability for voids : ø200 μm (when pixel size 300 μm) . Detectability for cracks: 20 μm x 5 mm (when pixel size 300 μm) . Accuracy for dimensional measurements: 100μm (pixel size 250 μm, zooming applied) . Minimum discernible density difference: 1 %			
Image proces-sing func-tions (for all models)	. Window processing . Addition and subtraction . Multiframe . Profile display . Converting section		. Measuring distance between two points . Zooming . Band display	

Table 2. Measuring conditions of residual stress in Si_3N_4/steel joint

CASE 1		CASE 2
Si_3N_4	S45C	Si_3N_4
RIGAKU PSPC Cr-Kα "V" filter 40kV, 35mA ϕ0.52mm		RIGAKU Cr-Kα "V" filter 50kV, 100mA ϕ0.38mm
(212) $2\theta_0$=131.47deg K=−90.08 kg/mm^2	(211) $2\theta_0$=156.1deg K=−32.44 kg/mm^2	(212) $2\theta_0$=131.47deg K=−90.08 kg/mm^2

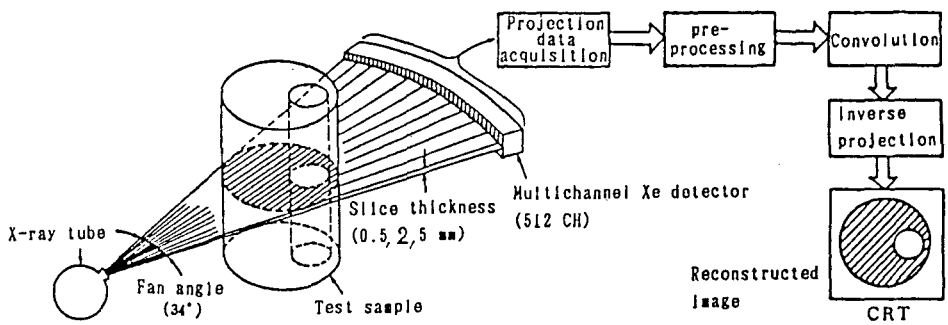

Figure 1. Schematic presentation of principle of the third generation CT scanner: from acquisition of projection data to reconstruction of image (TOSCANER-3000 Series)

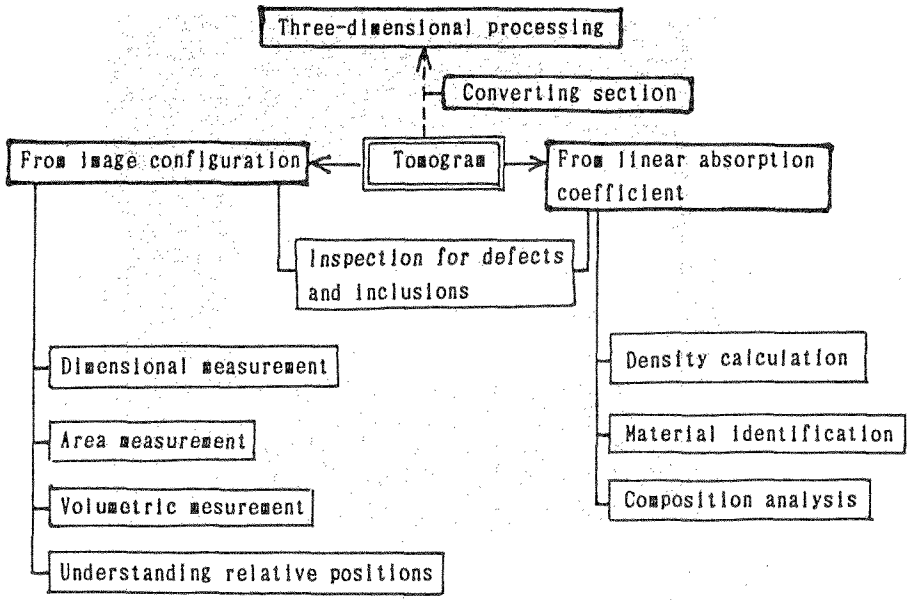

Figure 2. Information provided by tomogram

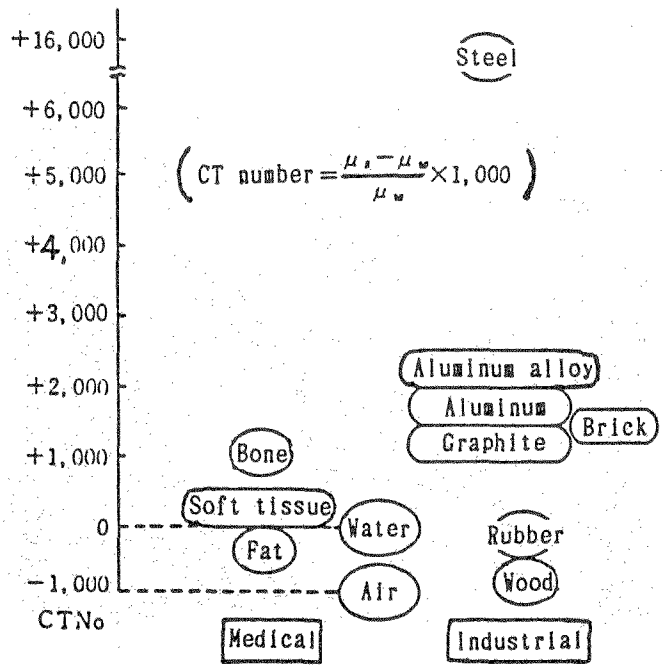

Figure 3. Relation between material - CT number

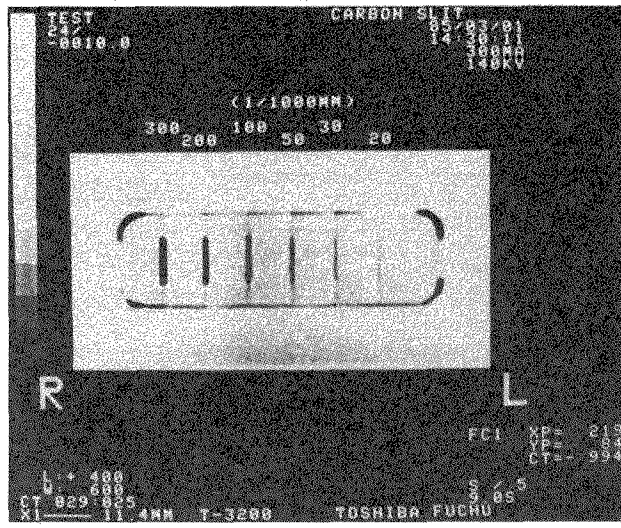

Figure 4. X-ray CT image of artificial slits in graphite (down to 20 μm in width)

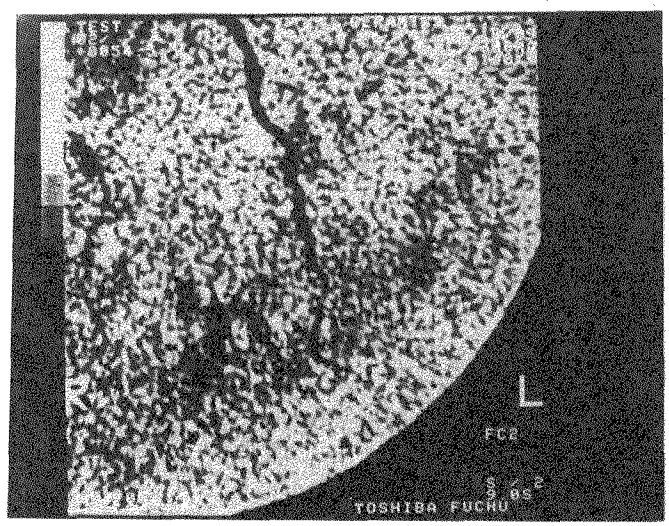

Figure 5. X-ray CT zoomed image of crack developed in mullite ceramics

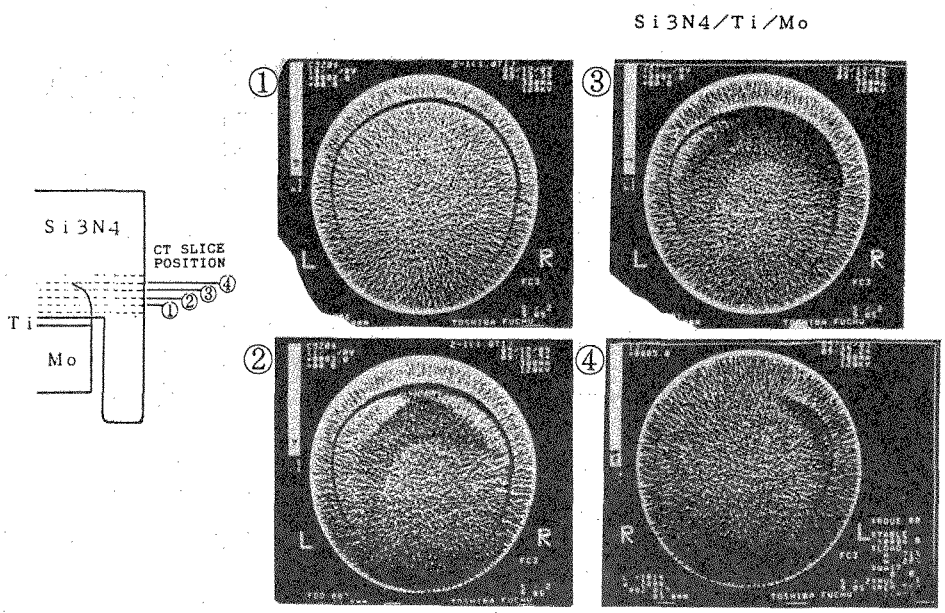

Figure 6. X-ray CT detection of crack introduced from the interface of Si_3N_4/Ti/Mo

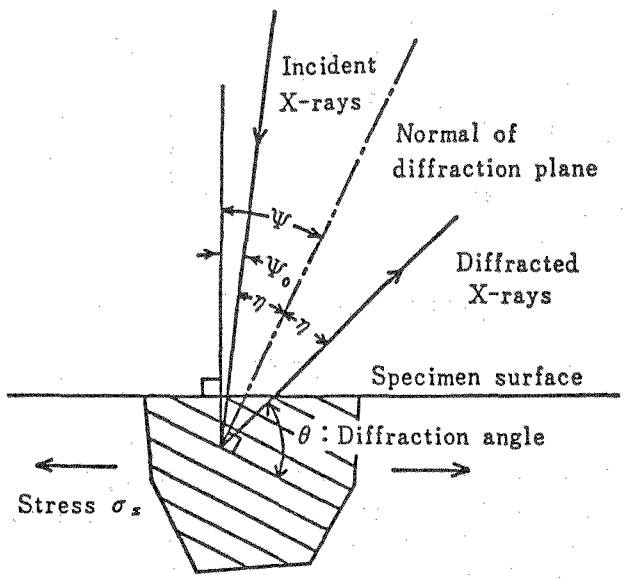

Figure 7. Principle of residual stress measurement by X-ray

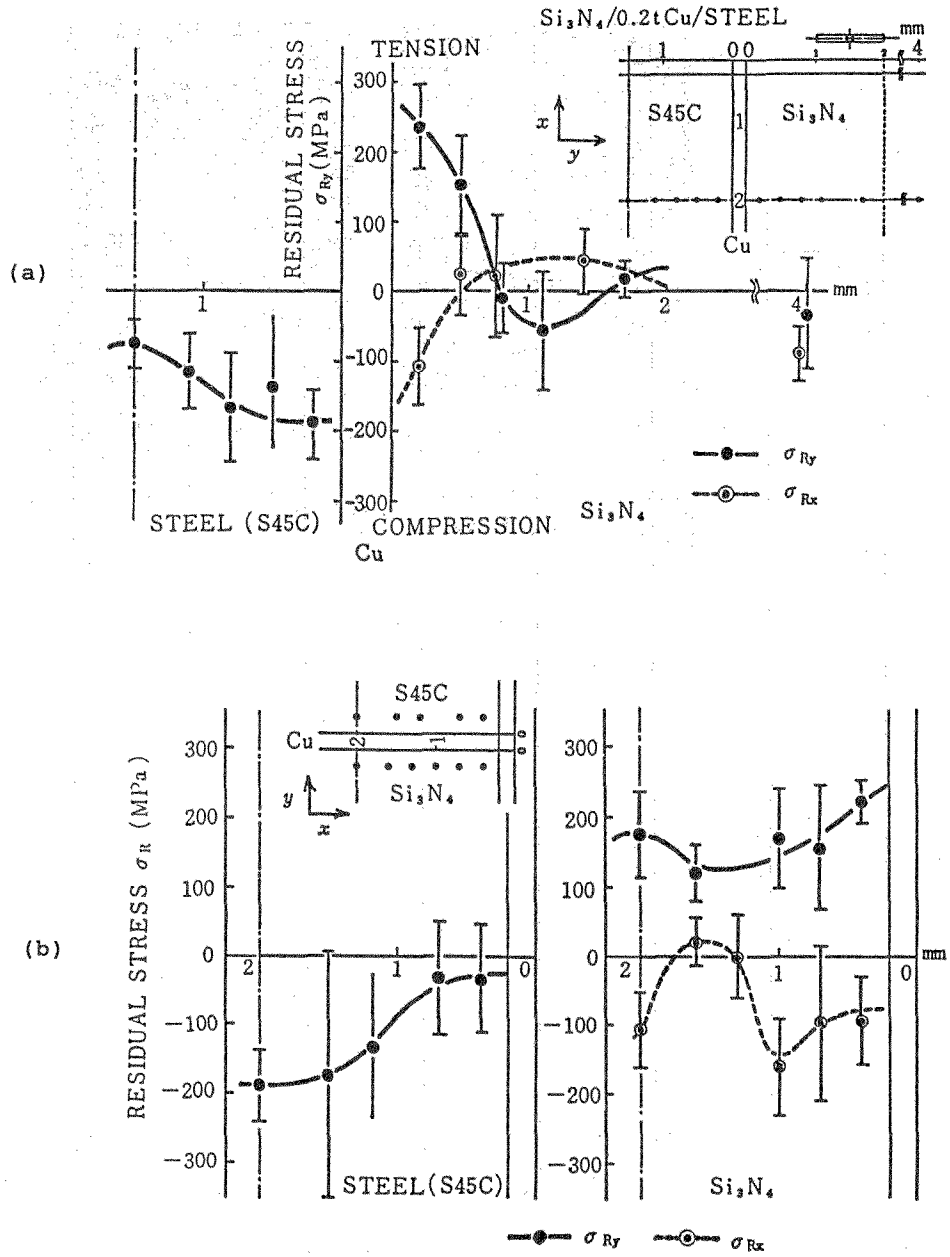

Figure 8. Residual stress distribution in Si_3N_4/0.2tCu/steel joint (3x4x40mm) measured by 0.3mmϕ collimated X-ray
(a) axial distributions
(b) distributions along interface

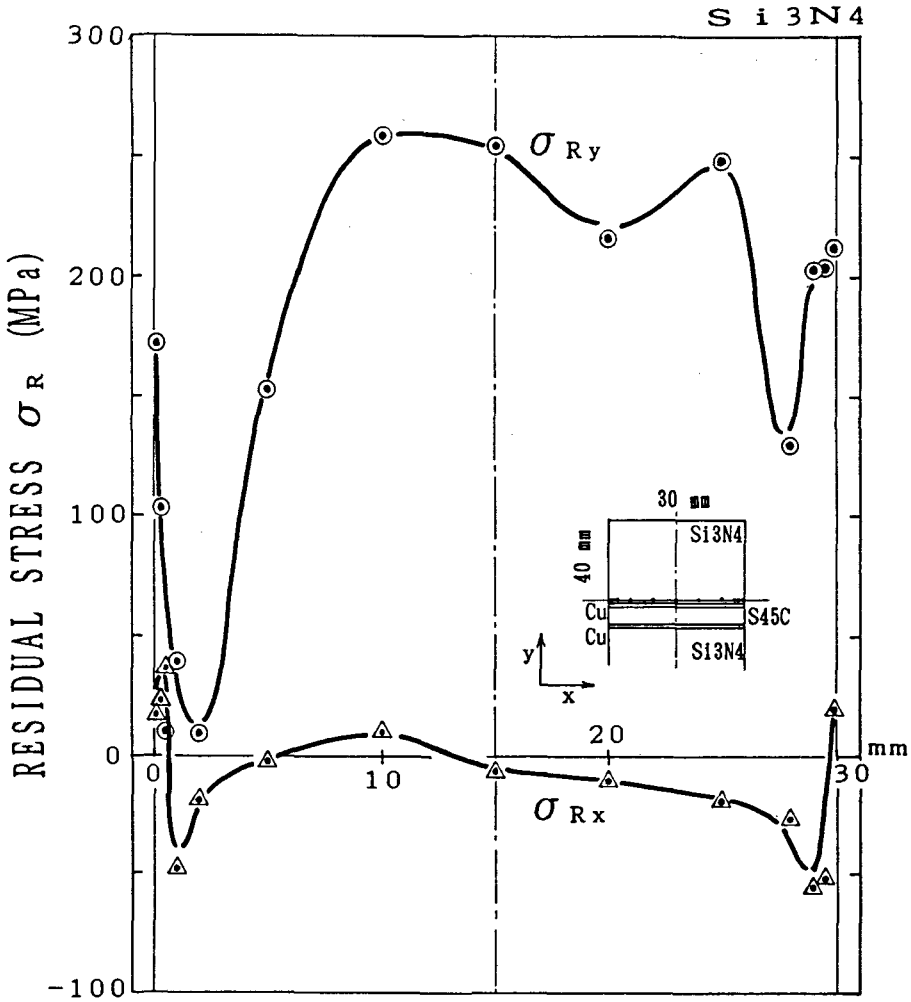

Figure 9. Residual stress distribution along interface in Si_3N_4/0.2tCu/steel joint (3x30x40mm) measured by 0.1mmϕ collimated X-ray